Inorg. Chem. **1998,** *37,* 1341−1346

α- and *β*-$CuAlCl_4$: Framework Construction Using Corner-Shared Tetrahedral Metal−Halide Building Blocks

James D. Martin,* Brian R. Leafblad, Roger M. Sullivan, and Paul D. Boyle

Department of Chemistry, North Carolina State University, Raleigh, North Carolina 27695

Received September 5, 1997

Rapid quenching of a melt of CuCl and $AlCl_3$ results in the formation of the metastable framework structure, β-$CuAlCl_4$. The structure, determined by single-crystal X-ray crystallography (space group $Pna2_1$, $a = 12.8388(5)$ Å, $b = 7.6455(3)$ Å, and $c = 6.1264(3)$ Å, $Z = 2$), can be derived from a distorted hexagonal closest packed anion sublattice. Annealing at temperatures above 100 °C results in a phase transition to the more thermodynamically stable α-$CuAlCl_4$. The solid solution $CuAlCl_{4-x}Br_x$ is described for both α and β phases. The structures of α-$CuAlCl_4$ and α-$CuAlBr_4$, determined by single-crystal X-ray diffraction (space group $P\bar{4}2c$, $a = b$ 5.4409(1) Å and $c = 10.1126(3)$ Å, $V = 299.37(1)$ Å^3, $Z = 2$, and $a = b = 5.7321(2)$ Å and $c = 10.6046(8)$ Å, $Z = 2$, respectively), are derived from a distorted cubic closest packed anion sublattice. The mechanism for this phase transition is described in relation to that previously described for cristobalite-type structures. The structures of both α- and β-$CuAlCl_4$ reveal large van der Waals channels, which are proposed to be important for the reversible adsorption of carbon monoxide and ethylene by these materials.

Introduction

Because of the strong Lewis acidic properties of $AlCl_3$, binary mixtures with other metal−halide salts have received considerable attention.[1] However, previous to this work, only one solid-state compound has been identified from the CuCl/$AlCl_3$ system.[2,3] The catalytic activity of the CuCl/$AlCl_3$ mixed−metal halide has been the subject of numerous investigations.[4] Cu(I) salts are also known to sorb carbon monoxide,[5] and mixtures of $CuAlCl_4$ with aromatic molecules have exhibited considerable utility in the separation of CO from other gas mixtures.[6] In addition, gas-phase studies of the CuCl/$AlCl_3$ system have indicated the likely presence of several $Cu_xAl_yCl_{x+3y}$ species.[7] We thought it might be possible to exploit the observed differential speciation of these mixed-metal halides in the gas phase in our synthetic pursuit of new metastable crystalline phases.

Structural studies of the copper aluminum halides are rather sparse, with only two crystal structures reported, including the structure of α-$CuAlCl_4$[3a] (α-$CuAlBr_4$[3b] and α-$CuGaCl_4$[8] are isosructural) and the compound $(C_6H_6)CuAlCl_4$.[9] The crystal structure of $CuGaI_4$ has also been reported.[10] Our interest in these copper aluminum halide materials stems from a recognition that these structures have been assembled from corner-sharing tetrahedral building units, reminiscent of silicate-type constructions. Given the utility of metal halides in organic synthesis and polymer chemistry, as solid electrolytes, and as optical materials, we have begun exploratory syntheses applying building-block construction principles to design novel metal−halide materials. We have already demonstrated that halozeotypes, of general formula $[Cu_nZn_{m-n}Cl_{2m}]^{n-}$, can be constructed yielding frameworks analogous to aluminosilicate zeolites.[11] Extending this zeolitic analogy, we propose that the copper aluminum halides will yield a family of $Cu_mAl_mCl_{4m}$ frameworks, analogous to the known family of aluminophosphates. We report here the synthesis and characterization of β-$CuAlCl_4$, the second solid-state compound isolated from the CuCl/$AlCl_3$ system, and describe the phase transition from β- to α-$CuAlCl_4$ and the small-molecule gas sorption properties. The construction of truly open framework metal−halide materials requires syntheses which employ molecular templates, as we have already demonstrated for the copper zinc halozeotypes. However, the structures of the α- and β-$CuAlCl_4$ demonstrate that even in the absence of templating species, frameworks constructed out of two types of tetrahedral building blocks of significantly different size can afford more "open" structures than an analogous structure constructed from a single building unit.

---

(1) *Ternary Alloys: A Comprehensive Compendium of Evaluated Constitutional Data and Phase Diagrams;* Petzow, G., Effenberg, G., Eds.; VCH: Weinheim, 1991; Vol. 4, pp 115−158.

(2) Kendall, J.; Crittenden, E. D.; Miller, H. K. *J. Am. Chem. Soc.* **1923**, *45*, 963.

(3) (a) Hildebrandt, K.; Jones, P. G.; Schwarzmann, E.; Sheldrick, G. M. *Z. Naturforsch.* **1982**, *37B*, 1129. (b) α-$CuAlCl_4$ and α-$CuAlBr_4$ by Rietveld analysis: Yamada, K.; Tomita, Y.; Okuda, T. *J. Mol. Struct.* **1995**, 219.

(4) (a) Johnson, B. H. (Esso Research and Engineering Co.) U.S. Patent 3475347, Oct. 28, 1969. (b) Walker, D. G. (Tenneco Chemicals, Inc.) Ger. Offen. 2057162, June 3, 1971. (c) Toshima, N.; Kanaka, K.; Koshirai, A.; Hirai, H. *Bull. Chem. Soc. Jpn.* **1988**, *61*, 2551. (d) Toniolo, L.; Graziani, M. *J. Organomet. Chem.* **1980**, *194*, 221.

(5) Hakansson, M.; Jagner, S. *Inorg. Chem.* **1990**, *29*, 5241.

(6) (a) Walker, D. G. *Prepr.*—*Am. Chem. Soc., Div. Pet. Chem.* **1983**, *28*, 746. (b) Hirai, H.; Nakamura, M.; Lomiyama, M. *Bull. Chem. Soc. Jpn.* **1983**, *56*, 2519. (c) Hirai, H.; Wada, K.; Komiyama, M. *Bull. Chem. Soc. Jpn.* **1986**, *59*, 1043. (d) Hirai, H.; Hara, S.; Komiyama, M. *Bull. Chem. Soc. Jpn.* **1986**, *59*, 1051.

(7) (a) Schäfer, H. *Adv. Inorg. Chem. Radiochem.* **1983**, *26*, 201. (b) Schäfer, H.; Rabeneck, H. *Z. Anorg. Allg. Chem.* **1978**, *443*, 28.

(8) Höenle, W. *Z. Kristallogr.* **1990**, *191*, 141.

(9) Turner, R. W.; Amma, E. L. *J. Am. Chem. Soc.* **1966**, *88*, 1877.

(10) Burus, R.; Zajonc, A.; Meyer, G. *Z. Kristallogr.* **1995**, *210*, 62

(11) Martin, J. D.; Greenwood, K. B. *Angew. Chem., Int. Engl. Ed.* **1997**, *36*, 2072.

Table 1. Lattice Constants for α- and β-CuMX$_4$ (Å)

	a	*c*		*a*	*b*	*c*
α-CuAlCl$_4$[a]	5.4409(1)	10.1126(3)	β-CuAlCl$_4$[a]	12.8388(5)	7.6455(3)	6.1264(3)
α-CuAlCl$_3$Br[b]	5.521(1)	10.197(5)	β-CuAlCl$_3$Br[b]	12.908(6)	7.684(4)	6.152(4)
α-CuAlCl$_2$Br$_2$[b]	5.607(1)	10.315(3)	β-CuAlCl$_2$Br$_2$[b]	13.161(6)	7.875(3)	6.296(3)
α-CuAlClBr$_3$[b]	5.6778(8)	10.469(2)	β-CuAlClBr$_3$[b]	13.199(7)	7.871(3)	6.292(3)
α-CuAlBr$_4$[a]	5.7321(2)	10.6046(8)				
α-CuGaCl$_4$[b]	5.415(1)	10.197(4)	β-CuGaCl$_4$[b]	12.900(11)	7.587(8)	6.153(4)
α-CuGaBr$_4$[b]	5.707(1)	10.669(5)				

[a] Lattice constants determined by single-crystal measurements on a CAD-4 diffractometer. [b] Lattice constants determined by powder X-ray diffraction using an Enraf-Nonius camera and Si as an internal standard.

Table 2. Crystallographic Data for β-CuAlCl$_4$ and α-CuAlBr$_4$

chemical formula	β-CuAlCl$_4$	α-CuAlBr$_4$
a, Å	12.8388(5)	5.7321(2)
b, Å	7.6455(3)	5.7321(2)
c, Å	6.1264(3)	10.6046(8)
V, Å^3	601.36(4)	348.44(3)
Z	4	2
fw	232.34	410.14
space group	*Pna*2$_1$ (No. 33)	$P\bar{4}2c$ (No. 112)
temp	20 °C	20 °C
λ(Mo Kα), Å	0.710 73	0.710 73
ρ_{calc}, g cm^{-3}	2.56	3.91
μ, cm^{-1}	54.4	258.7
R[a]	0.029	0.046
R_w[b]	0.038	0.047

[a] $R = \sum||F_o| - |F_c||/\sum|F_o|$. [b] $R_w = [\sum w(|F_o| - |F_c|)^2/\sum w|F_o|^2]^{1/2}$.

Results and Discussion

Synthesis. The mixed-metal halides, CuAlX$_4$ (X = Cl, Br) are readily synthesized in high yield from the melt of CuX and AlX$_3$ (<250 °C). (The α phase also can be synthesized by simply grinding the two starting materials together in a mortar and pestle.) Both α and β phases of CuAlX$_4$ are colorless crystalline solids that can be readily differentiated by X-ray powder diffraction (lattice constants are described in Table 1). Slow cooling of the melt to room temperature (25°/h) quantitatively yields crystalline α-CuAlX$_4$. By contrast, quenching the melt, sealed in a thin-walled fused-silica tube, by rapid immersion in an ice bath provides a quantitative yield of β-CuAlX$_4$. Single crystals of β-CuAlCl$_4$ were obtained from quenching a larger scale reaction run in a thick-walled fused-silica reaction vessel. Quenching under these reaction conditions provided a slightly slower cooling profile and yielded a mixture of well-formed rectangular prism single crystals of β-CuAlCl$_4$ and microcrystalline α-CuAlCl$_4$.

Similar preparations using the metal bromides or a mixture of the chlorides and bromides yield the full range of solid solutions, CuAlCl$_{4-x}$Br$_x$, with $x = 0-4$ for the α phase but only $x = 1-3$ for the β phase (see Table 1). No evidence of any superstructure due to Cl/Br ordering was observed. We have not yet been able to prepare the all bromide β-CuAlBr$_4$. The α phase of CuGaCl$_4$ was previously reported,[8] and we have synthesized β-CuGaCl$_4$ and α-CuGaBr$_4$. Interestingly, while the lattice constants expand in the expected fashion for the bromide/chloride substitution, the lattice constants for the Al and Ga species are nearly identical.

Structure Descriptions. The crystal structures of α-CuAlX$_4$ (X = Cl, Br) have been reported previously,[3] crystallizing in the tetragonal space group $P\bar{4}2c$ (No. 112). Crystallographic details for the single-crystal refinement of α-CuAlBr$_4$ are summarized in Table 2, and atomic positional parameters are given in Table 3. Structural details of α-CuAlX$_4$ are summarized later in the context of comparison with the new β-CuAlCl$_4$. The single-crystal structural refinement of α-CuAlCl$_4$ was previously reported by Sheldrick,[3a] and our single-crystal refinement of α-CuAlBr$_4$ is in agreement with the Rietveld structural solution previously reported by Yamada.[3b]

Table 3: Atomic Positional Parameters and Isotropic-Equivalent Displacement Parameters for CuAlX$_4$ Phases

	x	*y*	*z*	B_{iso}
β-CuAlCl$_4$				
Cu	0.33761(4)	0.9939(1)	0.05994	3.72(3)
Al	0.41292(8)	0.2475(1)	−0.4427(3)	1.92(5)
Cl1	0.40884(8)	0.2508(2)	−0.0934(3)	2.71(4)
Cl2	0.42943(8)	0.7443(2)	−0.0592(3)	2.81(4)
Cl3	0.33722(8)	0.0142(2)	0.4436(2)	3.00(5)
Cl4	0.16346(7)	0.9763(1)	−0.0661(3)	2.89(5)
α-CuAlBr$_4$				
Cu	$^1/_2$	$^1/_2$	0	2.76(6)
Al	$^1/_2$	0	$^1/_4$	1.44(15)
Br	0.2591(1)	0.2288(1)	0.12743(5)	2.05(3)

Table 4: Bond Distances and Bond Angles for CuAlX$_4$ Phases

β−CuAlCl$_4$			
Cu−Cl(1)	2.362(1)	Al−Cl(1)	2.141(3)
Cu−Cl(2)	2.359(1)	Al−Cl(2)	2.147(2)
Cu−Cl(3)	2.356(1)	Al−Cl(3)	2.147(2)
Cu−Cl(4)	2.369(1)	Al−Cl(3)	2.143(2)
Cl1−Cu−Cl2	110.88(5)	Cl1−Al−Cl2	110.79(9)
Cl1−Cu−Cl3	110.04(5)	Cl1−Al−Cl3	108.85(8)
Cl1−Cu−Cl4	106.44(5)	Cl1−Al−Cl4	109.37(8)
Cl2−Cu−Cl3	111.29(6)	Cl2−Al−Cl3	110.07(8)
Cl2−Cu−Cl4	108.96(5)	Cl2−Al−Cl4	106.87(8)
Cl3−Cu−Cl4	109.09(5)	Cl3−Al−Cl4	110.89(8)
Cu−Cl1−Al	113.39(6)	Cu−Cl3−Al	112.17(8)
Cu−Cl2−Al	110.17(7)	Cu−Cl4−Al	111.29(7)

	α-CuAlCl$_4$	α-CuAlCl$_4$
Cu−X	2.3605(8)	2.4797(6)
Al−X	2.1449(6)	2.3059(6)
X−Cu−X	112.72(3) × 2	113.96(2) × 2
	107.87(3) × 4	107.27(2) × 4
X−Al−X	110.53(4) × 2	111.37(2) × 2
	110.63(3) × 2	110.66(2) × 2
	107.28(3) × 2	106.42(2) × 2
Cu−X−Al	110.95(3)	109.28(3)

β-CuAlCl$_4$ crystallizes with orthorhombic *Pna*2$_1$ space group symmetry (No. 33). Crystallographic details for the single-crystal refinement of β-CuAlCl$_4$ are summarized in Table 2, and atomic positional parameters are given in Table 3. The lower crystal symmetry of the β phase removes the ideal tetrahedral symmetry from both the CuCl$_{4/2}$ and AlCl$_{4/2}$ building units such that around each tetrahedron the four M−Cl distances and six Cl−M−Cl angles are distinct (see Table 4) with average values of Cu−Cl = 2.361 Å, Cl−Cu−Cl = 109.45°, Al−Cl = 2.144 Å, and Cl−Al−Cl = 109.47°. More interesting is the structural result of framework construction using tetrahedral building units with distinctly different sizes (ΔM−X = 0.22 Å = $d_{\text{Cu−X}} - d_{\text{Al−X}}$). This effect is most visible in the inter-tetrahedral nonbonded contacts discussed below. The mis-

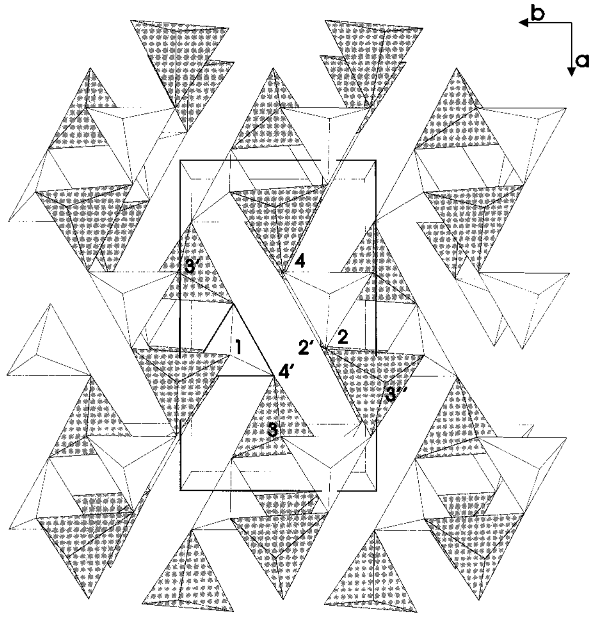

Figure 1. Polyhedral view of β-$CuAlCl_4$ looking down *c* and indicating the atom labeling scheme. Cu tetrahedra are shaded, and Al tetrahedra are not. Selected intertetrahedral Cl−Cl distances (Å) include Cl(1)−Cl(2) = 3.788(2), Cl(1)−Cl(2′) = 3.876(2), Cl(1)−Cl(3) = 3.753(1), Cl(1)−Cl(3′) = 3.845(2), Cl(1)−Cl(4) = 3.882(1), Cl(1)*−Cl(4′) = 3.777(2), Cl(2)−Cl(3) = 3.849(2), Cl(2)−Cl(3″)* = 3.865(2), Cl(2)−Cl(4′) = 3.840(2), Cl(2′)−Cl(4′) = 3.907(2), Cl(3)*−Cl(4′) = 3.753(2), and Cl(3′)−Cl(4) = 4.113(2).

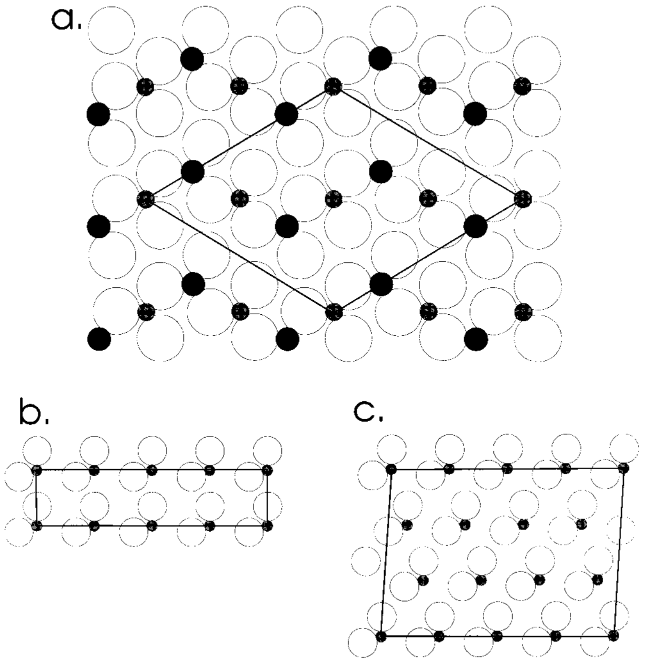

Figure 2. Description of the pseudo-closest packing in α- and β-$CuAlCl_4$. (a) A closest packed anion layer (001 slice of β-$CuAlCl_4$ and 112 slice of α-$CuAlCl_4$) indicating the cation ordering into 2 × 2 zigzag chains. The small gray spheres represent Al, and the larger black spheres represent Cu. A pseudohexagonal unit cell is outlined. (b) View of a "110" section of the pseudohexagonal cell of β-$CuAlCl_4$ emphasizing the hexagonal closest packing (010 slice of the real orthorhombic unit cell). (c) View of a "110" section of the pseudohexagonal cell of α-$CuAlCl_4$ emphasizing the cubic closest packing (110 slice of the real tetragonal unit cell).

matched sizes of the copper and aluminum tetrahedra also result in a slightly larger distortion from ideality for the larger $CuCl_{4/2}$ tetrahedra.

In β-$CuAlCl_4$, the $CuCl_{4/2}$ and $AlCl_{4/2}$ tetrahedra are connected through their corners (chloride bridges) into a three-dimensional framework structure shown in Figure 1. This extended structure can be described as a vacancy derivative of wurtzite, ZnS, in which only one-fourth of the tetrahedral sites are occupied within a distorted hexagonal closest packed (...ABA...) halide sublattice (Figure 2). The cations effectively break up the closest packed layers into snaking chains of alternating $CuCl_{4/2}$ and $AlCl_{4/2}$ corner sharing tetrahedra which run along *a*. This chainlike structure is indicative of significant covalent bonding character in the framework. The layers of chains are further connected into a three-dimensional network by corner sharing between closest packed layers. The cation ordering within a given layer creates vacancies which can be described as "van der Waals channels" between these snaking chains. In addition, the cation chains of the A and B layers are stacked around a 2_1 axis which creates an additional set of "van der Waals channels" running along *c*.

These van der Waals channels running along the *a* and *c* axes are constructed with 6-ring and 8-ring orifices, respectively. The 6-rings of the snaking channels connect the 8-ring channels, thus creating a 2-D channel network. The orifices, however, are not perpendicular to the channel direction, resulting in a small free diameter. The mismatched sizes of the copper− and aluminum−halide tetrahedra effectively distort the halide sublattice such that the intertetrahedral Cl−Cl contacts (ranging from 3.75 to 4.11 Å) are significantly larger than the intratetrahedral Cl−Cl contacts (3.50 Å and 3.85 Å for the Al and Cu tetrahedra, respectively). This corresponds to cross-channel Cl−Cl contacts of up to about 0.7 Å larger than the sum of chloride van der Waals radii (1.7 Å). The 8-ring channels running along *c* have a free diameter of 0.4 Å (Cl(2)−Cl(4) = 3.79 Å) across the shortest cross-channel contact and 8.3 Å (Cl(4)−Cl(4) = 11.71 Å) along the widest dimension. The height of the snaking channels running along *a* is equivalent to the *c* lattice constant, 6.13 Å (free diameter of 2.67 Å), while the width varies from Cl(1)−Cl(3) = 3.75 Å to Cl(3)−Cl(4) = 4.11 Å (free diameters of 0.4 and 0.7 Å, respectively). The shortest cross-channel halide−halide contacts cut the 6-ring orifice. The free diameters of these van der Waals channels can be compared with the free distance between van der Waals layers in MoS_2 = 0.06 Å (S−S = 3.66 Å)[12] and ZrCl = 0.2 Å (Cl−Cl = 3.61 Å).[13]

Although these van der Waals channels are too small to consider this system microporous, it is interesting to compare the structure of β-$CuAlCl_4$ to that of $AgZnPS_4$ in which silver cations are "stuffed" into the snaking channels of a $ZnPS_4^-$ framework.[14] These frameworks are isotypic, and their nearly identical lattice constants suggest that this framework is well suited toward the incorporation of small guests (note that Cl^- and S^{2-} anions are quite similar in size). In addition, the structure of β-$CuAlCl_4$ is an analogue of "*Pna*2_1 cristobalite."[15] The cristobalite framework is known to be somewhat flexibile,[16] and several stuffed cristobalite-type structures are reported.[17] Evidence for an interaction of this channel structure with guest molecules is found in the adsorption of small molecule gases.

---

(12) Wyckoff, R. W. G. *Crystal Structures*, 2nd ed.; Wiley: New York, 1963; Vol. 1, p 280.

(13) Adolphson, D. G.; Corbett, J. D. *Inorg. Chem.* **1976**, *15*, 1820.

(14) Toffoli, P.; Rouland, J. C.; Khodadad, P.; Rodier, N. *Acta Crystallogr.* **1985**, *C41*, 645.

(15) O'Keeffe, M.; Hyde, B. G. *Acta Crystallogr.* **1976**, *B32*, 2923.

(16) Yeganeh-Haeri, A.; Weidner, D. J.; Parise, J. B. *Science* **1992**, *257*, 650.

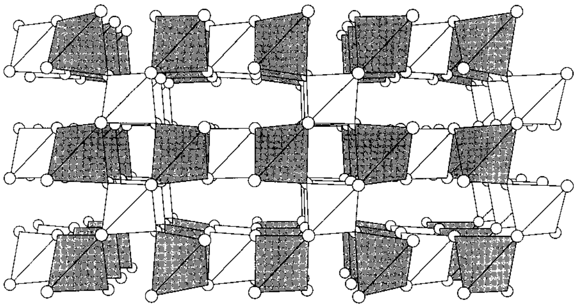

Figure 3. Polyhedral view of α-$CuAlX_4$ looking down. Cu tetrahedra are shaded, buy Al tetrahedra are not.

In a manner similar to that observed for other Cu(I) salts,[5] upon exposure to small-molecule gases, such as carbon monoxide or ethylene, both α- and *β*-$CuAlCl_4$ adsorb 0.5−1 equiv of gas per formula unit by gravimetric analyses. Exposure to ethylene for longer periods of time resulted in a greater uptake due to olefin polymerization. This adsorbed gas is also readily removed, as determined gravimetrically, upon heating to 100 °C or by moderate vacuum. However, as noted below, the reversible gas sorption results in a phase transition from the *β* to the α phase. A previous report also indicates that for the polymerization of ethylene by $CuAlCl_4$ and $(C_2H_5)AlCl_2$ "...an unusual ability to produce straight chain dimers and trimers..." is observed.[4a] We believe that these channels, in addition to a flexibility of this framework, may be responsible for this observed small-molecule adsorption and catalytic selectivity.

***β*-CuAlCl₄ to α-CuAlCl₄ Phase Transition.** Annealing a sample of *β*-$CuAlCl_4$ overnight at 100 °C results in a quantitative conversion to the α phase. Similarly, when the adsorbed gas (see above) is removed under vacuum, one is left with completely the α phase. The reverse of this phase transition (α to *β*) was never observed when samples equilibrated at temperatures below the melt were quenched. Thus we believe that the *β* phase is a kinetically trapped metastable phase. When the *β*-$CuAlCl_4$ to α-$CuAlCl_4$ phase transition was followed by differential scanning calorimetry (DSC), a small endotherm was observed with an onset of 96 °C previous to the melt at 236 °C.

To begin to understand this phase transition, it is important to recognize that whereas the *β* phase of $CuAlCl_4$ is constructed from cation ordering in one-fourth of the tetrahedral holes in a pseudohexagonal closest packed halide sublattice, the α phase is constructed from the same pseudo closest packed layers but stacked in a cubic closest packed fashion (Figure 2). In the α phase the ordering of the layers of closest packed halides and the cation zigzag chains requires a stacking sequence of ...Aa′Bb′Cc′Aa″Bb″Cc″Aa′..., in which each layer of zigzag chains is shifted by $^1/_6$, $^2/_6$, $^1/_6$ in the pseudohexagonal cell of the ccp lattice. This 6-fold stacking sequence is determined by the aluminum positions as the copper positions stack with a three-layer repeat. The stacking of the zigzag chains in the α phase results in the formation of an orthogonal set of large van der Waals channels shown in Figure 3. These, along with the intralayer zigzag channels, provide a three-dimensional van der Waals channel structure with dimensions very similar to those observed in the *β* phase. The existence of both ccp, and hcp, polymorphs of a material is quite common and is in fact also observed for α-$ZnCl_2$, ccp,[18] and orthorhombic $ZnCl_2$, hcp.[19] As noted above, the $CuAlX_4$ species are isoelectronic to $ZnCl_2$; however, the construction using two types of tetrahedral building units of mismatched size results in a 2 × 2 instead of a 1 × 1 repeat in the zigzag chains and, thus, larger van der Waals channels than are observed for $ZnCl_2$. Interestingly, the cation arrangement in $CuGaI_4$ where the ΔM−X distance is 0.06 Å is identical to that observed for $ZnCl_2$, where as $CuGaCl_4$ where ΔM−X is 0.18 Å is isostructural to $CuAlCl_4$.

The hcp/ccp phase transition between zinc blende and wurtzite-type structures has been extensively studied.[20] The most straightforward description of this transition involves a slippage of the closest packed layers via a martensitic-type transformation (a shearing mechanism between closest packed layers with no diffusion of ions). Such transformations generally occur over a broad temperature range and result in the observation of a variety of polytypes arising from different stacking sequences along the fcc ⟨111⟩ stacking direction.[20b] By contrast, α-$ZnCl_2$ and orthorhombic $ZnCl_2$ are derivatives of the C9 structure type ("high cristobalite" and "*Pna*2₁ cristobalite", respectively), which can be interrelated simply by rotation about two noncollinear axes, which each contain one of the $\bar{4}$ axes of the tetrahedra, as described by O'Keeffe and Hyde.[15] This latter structural interconversion, depicted in Figure 4b, can be accomplished completely without distorting any tetrahedra or breaking any bonds. While our $CuAlCl_4$ materials are structural analogues of the zinc chlorides, this latter type of phase transition is not possible given the connectivity imposed by the two different sizes of tetrahedral framework building units. Interestingly, ^{63}Cu and ^{27}Al NMR and ^{35}Cl NQR studies of α-$CuAlX_4$ (X = Cl, Br) by Yamada *et al.*[3b] give indication of Cu ion mobility with an onset around 107 °C. This is well below the temperature reported for reorientation of the aluminate ions, which is approximately 180 °C for $AlBr_4^-$. Copper ion diffusion alone cannot convert the α phase to the *β* phase since an anion rearrangement is required to transform an hcp anion sublattice to a ccp sublattice. Similarly, a layer slippage mechanism cannot account for the significantly different temperatures for copper and aluminum mobility. Because the *β* to α phase transition is observed at approximately the temperature reported for Cu ion mobility but below the temperature of aluminate reorientation, we propose a mechanism by which (1) half of the Cu ions migrate within a given layer, resulting in a $ZnCl_2$-type lattice (Figure 4a), such that (2) the *β* and α phases can be interconverted by simple torsion of the corner-connected tetrahedra (Figure 4b), followed by (3) diffusion back to sites more suited to the mismatched size of the $CuCl_{4/2}$ and $AlCl_{4/2}$ tetrahedra (Figure 4a). The structures of Na_2ZnSiO_4[21] and $CuGaI_4$[10] adopt the proposed intermediate (or transition state) structures, adding support to this mechanism. Studies to identify this intermediate are in progress.

Upon the adsorption and removal of the small-molecule gases such as CO and ethylene, noted above, we also observe the *β* phase to be completely converted to the more thermodynamically stable α phase. This reversible adsorption of gases and the corresponding phase transition occur readily at room temperature, implying yet a different mechanism for the phase transition. Nevertheless, the flexibility of this framework is

---

(17) For example, see: (a) Kitazawa, T.; Kikuyama, T.; Takeda, M.; Iwamoto, T. *J. Chem. Soc., Dalton Trans.* **1995**, 3715. (b) Frostang, S.; Grins, J.; Loueer D.; Werner, P. F. *Solid State Ionics* **1988**, *31*, 131.

(18) Brehler, B. *Z. Kristallogr.* **1961**, *115*, 373.

(19) Yakel, H. L.; Brynestad, J. *Inorg. Chem.* **1978**, *17*, 3294.

(20) (a) O'Keeffe, M.; Hyde, B. G. *Philos. Trans. R. Soc. London, Ser. A* **1980**, *295*, 553. (b) Rai, K. N. *Acta Crystallogr.* **1971**, *A27*, 206. (c) Bol'shakov, A. F.; Dmitrenko, A. O.; Abalduev, B. V. *Izv. Akad. Nauk SSSR Neorg. Mater.* **1979**, *15*, 1528. (d) Plyusnin, A. B.; Dubrovina, A. N.; Finarev, M. S. *Sov. Phys. Crystallogr.* **1979**, *24*, 344.

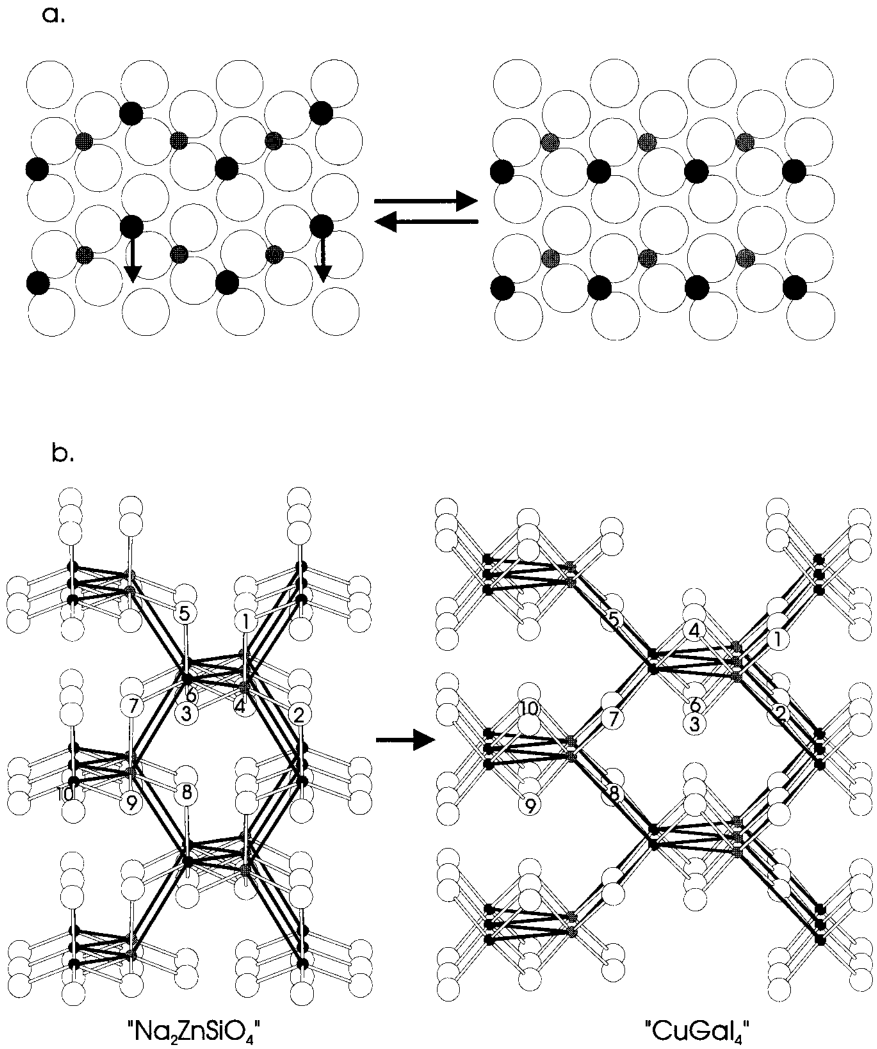

Figure 4. Representation of the proposed β to α phase transition in $CuAlCl_4$. (a) Description of the Cu ion migration required to convert the "closest packed layers" of α- and β-$CuAlCl_4$ to that of the $CuGaI_4$- and Na_2ZnSiO_4-type "closest packed layers." (b) Ball and stick representation of the cristobalite-related hcp and ccp $MM'X_4$ structures that can be interconverted by twisting of the constituent tetrahedra. The metal−metal connectivity is highlighted to emphasize the identical connectivity of these frameworks. Ten of the anions are numbered to articulate the structural reorientation.

expected to be responsible for both the β to α phase transition and the ability to absorb small molecule gases into channels that are theoretically too small for the guest molecules. Further studies to understand the adsorption of gases into these novel frameworks are in progress.[22]

Experimental Section

General Procedures. All reactions were performed under inert atmosphere conditions in a N_2-filled glovebox or on vacuum or Schlenk lines. $AlCl_3$ was purchased from Fluka and purified by literature procedures.[23] CuCl was prepared from Cu metal and $CuCl_2$ (Aldrich) according to literature methods.[24] CuBr, $AlBr_3$, $GaCl_3$, and $GaBr_3$ were purchased from Aldrich and purified by sublimation. CO and ethylene were purchased from National Welders and used after passage through a drying column of 4 Å molecular sieves. All powder X-ray diffraction measurements were obtained using an Enraf-Nonius Guinier camera and were indexed with respect to a silicon standard.

Syntheses. (a) α-$CuAlCl_4$. A 0.49 g (5 mmol) amount of CuCl and 0.67 g (5.0 mmol) of $AlCl_3$ were ground together with a mortar and pestle and placed into a Pyrex ampule under N_2. The ampule was then evacuated (0.5 mTorr) and flame-sealed. The reaction tube was heated to 250 °C, melting the reactants. The furnace was then turned off and allowed to cool to ambient temperature, yielding pure crystalline α-$CuAlCl_4$. This material can be further purified by sublimation by allowing one end of the Pyrex tube to extend outside the tube furnace. However, upon sublimation some crystalline $AlCl_3$ is almost always observed, indicating some disproportionation into CuCl and $AlCl_3$.

(b) β-$CuAlCl_4$. A 100 mg (0.43 mmol) amount of α-$CuAlCl_4$ was placed in a 1.0 mm walled fused silica tube which was then evacuated and flame-sealed. The reaction vessel was then heated to 250 °C until the material melted. The reaction vessel was then plunged into an ice bath to quench the reaction mixture, resulting in a quantitative yield of β-$CuAlCl_4$. Larger scale reactions and reactions in fused-silica tubes

---

(21) Joubert-Bettan, C. A.; Lachenal, R.; Bertaut, E. F. Parthe, E. *J. Solid State Chem.* **1969**, *1*, 1.

(22) The ethylene adduct has to date been the most amenable to study by X-ray diffraction. Four of the characteristic lines for the ethylene adduct are as follows, with *d* in Å (% intensity): 6.274 (100), 5.595 (70), 3.646 (15), and 3.046 (70), which can be indexed to a tetragonal cell $a = b = 6.299(3)$ Å and $c = 11.99(1)$ Å. Lines consistent with a $\sqrt{2} \times \sqrt{2}$ superstructure are observed upon longer exposure to ethylene.

(23) (a) Wilkes, J. S.; Levisky, J. A.; Wilson, R. A.; Hussey, C. L. *Inorg. Chem.* **1982**, *21*, 1263. (b) Gale, R. J.; Osteryoung, R. A., In *Molten Salt Techniques*; Lovering, D. G., Gale R. J., Eds.; Plenum: New York, 1983; Chapter 3.

(24) Kauffman, G. B.; Fang, L. Y. *Inorg. Synth.* **1983**, *22*, 101.

with wall diameters of greater than 1 mm generally yield a mixture of the α and *β* phases.

(c) $CuAlCl_{4-x}Br_x$. Mixed-halide materials were prepared for both the α and the *β* phases according to the above methods using CuCl, CuBr, $AlCl_3$, and $AlBr_3$, respectively.

X-ray Structural Determination. (a) Crystal Structure Analysis of *β*-$CuAlCl_4$. A colorless single crystal of *β*-$CuAlCl_4$ (0.3 × 0.1 × 0.05 mm) was sealed within a 0.3 mm Pyrex capillary under dry nitrogen. Lattice constants, $a = 12.8388(5)$ Å, $b = 7.6455(3)$ Å, and $c = 6.1264(3)$ Å, $V = 601.36(4)$ Å^3, were obtained from centering 24 reflections $36 < 2\theta < 41°$, $Z = 4$. Systematic absences were consistent with the orthorhombic space group $Pna2_1$ (No. 33), which was confirmed in the subsequent refinement. Lattice constants and systematic absences were confirmed by zero- and first-layer Weissenberg photographs. Data were collected on an Enraf-Nonius CAD-4 diffractometer at 22 °C with monochromated Mo Kα radiation, ($\pm h$, $\pm k$, $\pm l$, $0 < 2\theta < 50°$). The structure was solved using SIR92 and refined using the NRCVAX programs.[25] The residuals were $R(F) = 0.029$, $R_w = 0.038$ for 943 independent reflections $2\theta < 50°$, $I > 0.5\sigma(I)$, and 55 variables. The rectangular prismatic crystal required no absorption correction ($\mu = 54.4$ cm^{-1}). It was not possible to refine the absolute structure due to the pervasive pseudosymmetry occurring in the Cl, Cu, and Al sublattices.

(b) Crystal Structure Analysis of α-$CuAlBr_4$. A colorless single crystal of α-$CuAlBr_4$ (0.35 × 0.4 × 0.25 mm) was sealed within a 0.3 mm Pyrex capillary under dry nitrogen. Lattice constants, $a = b = 5.7321(2)$ Å and $c = 10.6046(8)$ Å, $V = 348.44(3)$ Å^3, were obtained from centering 24 reflections $31 < 2\theta < 38°$, $Z = 2$. Systematic absences were consistent with the tetragonal space group $P\bar{4}2c$ (No. 112) which was subsequently confirmed in the final refinement. Data were collected on an Enraf-Nonius CAD-4 diffractometer at 22 °C with monochromated Mo Kα radiation, ($\pm h$, $\pm k$, $\pm l$, $0° < 2\theta < 60°$). The structure was solved using SIR92 and refined using the NRCVAX programs.[25] The residuals were $R(F) = 0.046$, $R_w = 0.047$ for 425 independent reflections $2\theta < 60°$, and 17 variables. An empirical absorption correction derived from ψ scans of several reflections was applied to all data ($\mu = 259$ cm^{-1}). The Rogers chirality parameter was refined to a value of 0.9(1), confirming the absolute configuration.

(c) *β*-$CuAlCl_4$ to α-$CuAlCl_4$ phase transition. Samples of *β*-$CuAlCl_4$ (10−20 mg) were placed into hermetically sealed high-pressure, gold-lined DSC capsules in a nitrogen-filled glovebox. The sample was transferred to a Perkin-Elmer DSC7 instrument and heated at a rate of 10 °C/min from room temperature to 300 °C.

Samples of *β*-$CuAlCl_4$ were loaded in to 0.5 mm quartz capillaries, heated for 24 h at 50, 75, 100, and 125 °C, and then quenched to room temperature. The capillaries were then transferred to an Enraf Nonius X-ray Guinier powder camera. Powder patterns were then analyzed for the presence of α- or *β*-$CuAlCl_4$.

Samples of 100 mg of α-$CuAlCl_4$ and *β*-$CuAlCl_4$ were sealed into fused-silica tubes and then heated to 100, 125, 150, 175, 200, and 225 °C (±1 °C), respectively, for 24 h and then quenched into an ice bath. X-ray powder patterns were taken of these samples to determine the product composition.

Gas Sorption. Samples of approximately 20 mg (0.086 mmol) of α- or *β*-$CuAlCl_4$ were placed onto a platinum TGA pan under a flowing stream of dry nitrogen (20 psi supply to instrument) on a Perkin-Elmer TGA7. The sample was then exposed to a stream of CO or C_2H_4 (20 psi supply to instrument) in addition to the nitrogen carrier gas. When no more gas was being adsorbed, the sample gas was shut off and the sample was heated to 100 °C under a stream of dry nitrogen to drive off the adsorbate. The identity of the final product was confirmed by powder X-ray diffraction.

Alternatively, 100 mg (0.43 mmol) samples of α- or *β*-$CuAlCl_4$ were placed in a reaction vessel that could be opened to a gas line. The loaded reaction vessel, closed under 1 atm of N_2, was carefully weighed on an analytical balance. The reaction vessel was then open to 1 atm of CO or C_2H_4 gas for 1−12 h and then weighed again to determine the gas uptake. After exposure to moderate vacuum (0.1 Torr) or standing overnight in a nitrogen-filled glovebox, all samples that had been exposed to CO or C_2H_4 were observed to be completely converted back to α-$CuAlCl_4$, as determined by Guinier X-ray powder diffraction.

Acknowledgment. The authors gratefully acknowledge Dr. C. B. Gorman for use of the TGA and DSC instrumentation. This work was supported by the National Science Foundation, CAREER award (DMR-9501370), and by an instrumentation grant (CHE-9509532).

Supporting Information Available: Two crystallographic files in CIF format are available on the Internet only. Access information is given on any current masthead page.

IC971148V

---

[25] Gabe, E. J.; Le Page, Y.; Charland, J.-P.; Lee, F. L.; White, P. S. *J. Appl. Crystallogr.* **1989**, *22*, 384.